

Tracing the Early Development of Harmful Algal Blooms on the West Florida Shelf with the Aid of Lagrangian Coherent Structures

M. J. Olascoaga,¹ F. J. Beron-Vera,¹ L. E. Brand,¹ and H. Koçak²

M. J. Olascoaga, F. J. Beron-Vera and L. E. Brand, RSMAS/AMP, University of Miami, 4600 Rickenbacker Cswy., Miami, FL 33149, USA. (jolascoaga@rsmas.miami.edu)

H. Koçak, Departments of Computer Science and Mathematics, University of Miami, 1365 Memorial Dr., Coral Gables, FL 33124, USA.

¹Rosenstiel School of Marine and Atmospheric Science, University of Miami, Miami, Florida, USA.

²Departments of Computer Science and Mathematics, University of Miami, Miami, Florida, USA.

arXiv:0708.4198v1 [physics.ao-ph] 30 Aug 2007

Abstract. Several theories have been proposed to explain the development of harmful algal blooms (HABs) produced by the toxic dinoflagellate *Karenia brevis* on the West Florida Shelf. However, because the early stages of HAB development are usually not detected, these theories have been so far very difficult to verify. In this paper we employ simulated *Lagrangian coherent structures* (LCSs) to trace the early location of a HAB in late 2004 before it was transported to an area where it could be detected by satellite imagery, and then we make use of a population dynamics model to infer the factors that may have led to its development. The LCSs, which are computed based on a surface flow description provided by an ocean circulation model, delineate past and future histories of boundaries of passively advected fluid domains. The population dynamics model determines nitrogen in two components, nutrients and phytoplankton, which are assumed to be passively advected by the simulated surface currents. Two nearshore nutrient sources are identified for the HAB whose evolution is found to be strongly tied to the simulated LCSs. While one nutrient source can be associated with a coastal upwelling event, the other is seen to be produced by river runoff, which provides support to a theory of HAB development that considers nutrient loading into coastal waters produced by human activities as a critical element. Our results show that the use of simulated LCSs and a population dynamics model can greatly enhance our understanding of the early stages of the development of HABs.

1. Introduction

The largest and most frequent harmful algal blooms (HABs) caused by the toxic dinoflagellate *Karenia brevis* tend to occur along the southern portion of the West Florida Shelf (WFS) [Steidinger and Haddad, 1981; Kusek et al., 1999; Brand and Compton, 2007]. Associated with typical HAB events is widespread death of sea life resulting from the brevetoxins produced by *K. brevis* [Bossart et al., 1998; Landsberg and Steidinger, 1998; Landsberg, 2002; Shumway et al., 2003; Flewelling et al., 2005]. Brevetoxins are also known to cause injury to humans through ingestion of contaminated seafood, skin contact, or inhalation of aerosolized brevetoxins in coastal regions [Backer et al., 2003; Kirkpatrick et al., 2004].

Dinoflagellates have slow growth rates [Brand and Guillard, 1981]. As a result, a necessary condition for achieving a high dinoflagellate population density is that physical processes (stretching and folding of fluid elements) do not act to significantly reduce the population density during the growth phase. Indeed, dinoflagellate blooms often occur in enclosed basins. The tendency of *K. brevis* to cause large HABs along the southern WFS may then be explained by the presence of a cross-shelf transport barrier that has been revealed in the analysis of drifter trajectories [Yang et al., 1999] and in an appropriate synthesis of modeled surface currents [Olascoaga et al., 2006]. In Olascoaga et al. [2006] it was hypothesized that the presence of such a transport barrier, which was characterized as a *Lagrangian coherent structure* (LCS), provides favorable conditions for the development of HABs in the southern WFS by inhibiting cross-shelf transport and thereby allowing for a greater nutrient buildup. We remark that, being of a fundamentally Lagrangian nature,

the aforementioned transport barrier could not be identified visually from snapshots of the simulated surface velocity field.

Satellite ocean color sensors have demonstrated the ability to provide a very useful HAB monitoring capability [Tester *et al.*, 1998; Stumpf *et al.*, 2003; Tomlinson *et al.*, 2004; Hu *et al.*, 2005; de-Araújo-Carvalho *et al.*, 2007]. To be detectable by current satellite sensors, however, the *K. brevis* cell concentration must be of the order of 10^5 cell l^{-1} (equivalently 1 mg Chl m^{-3}) [Tester *et al.*, 1998], which may take a period of about one month from background concentration to be attained [Tester and Steidinger, 1997; Steidinger *et al.*, 1998]. As a consequence, satellite ocean color imagery by itself is not capable of detecting HAB initiation, and hence cannot be used to determine what factors favor HAB development, which is a subject of continuous debate.

Earlier work [Rounsefell and Nelson, 1966] has associated the development of HABs on the WFS with river runoff, pollution, and other nutrient enriching phenomena produced by human activities. Consistent with this earlier work and the increase in the frequency of HABs experienced during the last century, a recent study [Brand and Compton, 2007] has indicated that *K. brevis* concentrations are indeed higher near the shoreline than offshore, and that nutrient-rich freshwater runoff from land is likely to be a major source of nutrients for the development of HABs. Other investigators [Hu *et al.*, 2006] have argued that, in addition to river runoff, submarine groundwater discharge, particularly when enhanced by an active hurricane season, should play a role in stimulating HABs on the WFS. It has been also suggested [Tester and Steidinger, 1997] that some HABs initiate several tens of kilometers offshore, near frontal regions, and that upwelling events provide a mechanism for supplying the required nutrients for their stimulation. One further, more

complicated, theory has been proposed [Lenes *et al.*, 2001; Walsh and Steidinger, 2001; Walsh *et al.*, 2003; Walsh *et al.*, 2006] which explains HAB development as a sequence of events preceded by iron-rich Saharan dust deposition. In short, the theory assumes that the Saharan dust stimulates *Trichodesmium* blooms, which fix nitrogen. The blooms decompose on sinking and release dissolved organic nitrogen, which stimulates a *K. brevis* seed population near the bottom. Coastal upwelling is then required to help this population reaching the surface, where light inhibition is alleviated and a HAB finally develops. However, as already pointed out, the early stages of the development of HABs are usually not detected, which makes it very difficult to test the aforementioned theories.

The goal of this paper is to demonstrate the utility of simulated LCSs to help trace the early stages of the development of HABs, and consequently to help acquiring a better understanding of the environmental factors that may lead to their development. We focus on a HAB that was observed on the southern portion of the WFS during October–December 2004 (Figure 1) [Hu *et al.*, 2005]. Focus on this HAB is placed both because of good event coverage and because it preceded an anomalously active HAB season which extended over most of 2005. The HAB was detected offshore using MODIS (Moderate Resolution Imaging Spectroradiometer) fluorescence line height imagery. The remote sensing detected high concentrations of chlorophyll, and water sampling and microscopic counts confirmed that this HAB contained mostly *K. brevis*. The early location of this HAB is traced here using simulated LCSs, which carry critical information that highly constrain fluid particle motion. The environmental conditions that may have led to the development of the HAB in question are then inferred using a nutrient–phytoplankton population dynamics model. Our LCSs analysis and population dynamics modeling effort

are based on a simulation of the WFS produced by the HYbrid-Coordinate Ocean Model (HYCOM).

2. Lagrangian Coherent Structures

A practical way to identify LCSs consists in computing direct finite-time Lyapunov exponents (DFTLEs) [Haller, 2001, 2002; Shadden *et al.*, 2005; Lekien *et al.*, 2005; Shadden *et al.*, 2006; Mathur *et al.*, 2007; Lekien *et al.*, 2007; Green *et al.*, 2007]. The DFTLE is a scalar that measures the finite-time average of the maximum separation rate of pairs of passively advected fluid particles. More specifically, the DFTLE is defined as

$$\sigma_{t_0}^\tau(\mathbf{x}_0) := \frac{1}{|\tau|} \ln \|\partial_{\mathbf{x}_0} \mathbf{x}(t_0 + \tau; \mathbf{x}_0, t_0)\|, \quad (1)$$

where $\|\cdot\|$ denotes spectral norm and $\mathbf{x}(t_0 + \tau; \mathbf{x}_0, t_0)$ is the position at time $t_0 + \tau$ of a fluid particle that at time t_0 was located at \mathbf{x}_0 . The latter is obtained by integrating the particle trajectory equation

$$\dot{\mathbf{x}} = \mathbf{u}(\mathbf{x}, t), \quad (2)$$

where the overdot stands for time differentiation and $\mathbf{u}(\mathbf{x}, t)$ is the fluid velocity.

Regions of maximum material line stretching produce local maximizing curves or “ridges” in the DFTLE field. When the DFTLE is computed by integrating particle trajectories backward (forward) in time, $\tau < 0$ ($\tau > 0$), a ridge in the DFTLE field corresponds to an attracting (repelling) LCS. The repelling and attracting LCSs provide, respectively, a generalization of the concepts of stable and unstable manifolds of a hyperbolic (stagnation) point to the case of aperiodically time-dependent velocity fields. The attracting and repelling LCSs delineate, like a separatrix, the boundary between regions

with different flow characteristics which do not mix, and constrain, respectively, the past and future history of passively advected fluid particles.

Numerical model output provides a flow description $\mathbf{u}(\mathbf{x}, t)$ that is suitable for use in the identification of LCSs. In *Olascoaga et al.* [2006] we considered daily surface velocity fields extracted in the WFS domain from a $1/25^\circ$ -resolution, free-running HYCOM simulation of the Gulf of Mexico (GoM), itself nested within a $1/12^\circ$ -resolution Atlantic basin data assimilative nowcast, which was generated at the U.S. Naval Research Laboratory as part of the Global Ocean Data Assimilation Experiment [*Chassignet et al.*, 2007]. Using these surface currents, in *Olascoaga et al.* [2006] we identified LCSs on the WFS that revealed the presence of a cross-shelf transport barrier in approximately the same location as the western boundary of the “forbidden zone,” which is a region on the southernmost part of the WFS that was found not to be visited by drifters that were released outside of the region [*Yang et al.*, 1999]. A highly convoluted portion of the aforementioned transport barrier can be seen in Figures 2 and 3, which show on selected days in 2004 DFTLE field snapshots computed by integrating (2) backward in time, with $\tau = -60$ d. The portion of the cross-shelf transport barrier is identified in this figure as the DFTLE field ridges shown with intense red tones. To construct this and the subsequent figure we considered surface currents produced by a HYCOM simulation of the WFS which, unlike that considered in *Olascoaga et al.* [2006], assimilated during the period 2004–2005 satellite-derived sea surface height and temperature data, as well as available vertical profile data in the GoM using the U.S. Navy Coupled Ocean Data Assimilation system [*Cummings*, 2005; *Hogan et al.*, 2007]. The validity of the surface circulation produced by this HYCOM simulation is supported by a very good agreement of simulated LCSs with available drifter trajectories

on the dates of the simulation, which can be accessed at the NOAA's Atlantic Oceanographic and Meteorological Laboratory website <http://www.aoml.noaa.gov/sfros/drifters>, and, as shown below, the ability of the HYCOM simulation to produce surface currents which lead to a simulated HAB with similar characteristics as those of the event observed on the WFS in late 2004.

The focus in this paper is not on the above persistent, large scale LCS which constitutes a barrier that inhibits transport across the WFS. Rather, it is on other less persistent, smaller scale LCSs, which lie on the shoreward side of the more prominent cross-shelf transport barrier. The LCSs in question are identified in Figures 2 and 3 with the DFTLE field ridges with tones ranging from less intense red through most intense blue in the colorscale. Note, in particular, the presence of a banana-shaped region bounded by LCSs of the latter type. The banana-shaped region, which is most clearly evident on mid December 2004 but can be traced in time from late October 2004 (Figure 2), coincides remarkably well with the area spanned by the HAB described in *Hu et al.* [2005] on 13 December 2004 (Figure 1i). The noted agreement between modeled LCSs and the boundary of the observed HAB distribution is exploited in the following sections to trace the early development of the observed HAB.

3. Tracing the Early Development of the Harmful Algal Bloom

In this section we trace the early development of the HAB described in *Hu et al.* [2005] using the simulated LCSs, which, as explained above, carry critical information that strongly constrain fluid particle motion. We thus concentrate on the DFTLE fields shown in Figures 2 and 3. Depicted on these figures also are instantaneous particle positions com-

puted by integrating (2) using the same HYCOM-based flow description $\mathbf{u}(\mathbf{x}, t)$ employed in computing the DFTLE fields.

Consider first the particle positions lying within the aforementioned banana-shaped region that resembles the area occupied by the HAB in question on 13 December 2004 (Figure 2, right panel). Immersed in the cloud of particles, which are indicated with black dots, is one particle indicated with a bold magenta dot that was used for reference in tracing the early location of the observed HAB. We chose the position of this fiducial particle to lie approximately centered within the banana-shaped region on 13 December 2004. Integrating backward in time (2) during 30 d with this initial condition, we found that the the early location of the HAB distribution in question could have restricted to a nearshore area between Estero Bay and Cape Romano (Figure 2, left panel). The integration time was chosen so as to correspond to the time it typically takes for *K. brevis* to develop a HAB. Note that the fiducial particle remains for all dates shown in Figure 2 within the LCSs that delimit the banana-shaped region. The particle positions indicated with black dots were computed by integrating (2) forward in time during 30 d with initial positions surrounding that of the fiducial particle on 13 November 2004 in a nearshore region between Estero Bay and Cape Romano, which lies within the LCSs that bound the banana-shaped region on that date. Note that as time progresses from 13 November 2004 the particles fill the banana-shaped region while it stretches and bends. Note also that during the relevant time interval the particles approach, but do not traverse, the DFTLE ridges that bound the banana-shaped region, which provides strong support for our assertion that these DFTLE ridges are attracting LCSs.

Consider now the fiducial particle shown in the right panel of Figure 3. This fiducial particle was located in the center of the observed HAB distribution on 13 November 2004, which is situated north of the banana-shaped region in the DFTLE field on that date. Integrating (2) backward in time during 30 d with this initial position, we found that the early location of the HAB distribution in question could have restricted to an area near the mouth of the Caloosahatchee River (Figure 3, left panel). Integrating (2) forward in time during 30 d for a cloud of particles with initial positions surrounding that of the fiducial particle on 14 October 2004, we found that these particles approximately covered the area spanned by the observed HAB on 13 November 2004. We emphasize that the motion of the particles is completely determined by the underlying LCSs. Note, in particular, the LCS on 14 October 2004 which appears to originate in the Caloosahatchee River mouth area, right before the aforementioned banana-shaped region starts to develop. Clearly, particles initially located near the shoreline north of the Caloosahatchee River mouth will never enter the banana-shaped region. Contrarily, these particles will disperse over a region characterized by a highly intricate underlying LCS.

In the following section we consider a simplified population dynamics model which reproduces the observed HAB's main characteristics. The population dynamics model considers initial nutrient sources located in the two regions of potential early HAB development estimated above based on the information contained in the modeled LCSs.

4. Population Dynamics Model

A number of biological and physical factors contribute to the initiation, growth, maintenance, and demise of HABs produced by *K. brevis*. We consider nutrient supply and surface ocean circulation constraints as the most important factors.

Consistent with these assumptions, we formulate a population dynamics model in which the nitrogen concentration is determined in two compartments, nutrients (N) and phytoplankton (P), which is partly justified by the lack of *K. brevis* grazers [Steidinger, 1973]. We further assume that these densities are passively advected by surface currents, which are described by the HYCOM simulation of the WFS. The equations describing the evolution of N and P take the form [Riley, 1963; Wroblewski and O' Brien, 1976; Wroblewski et al., 1988]

$$\partial_t N + \mathbf{u} \cdot \nabla N = -\mu \frac{N}{N + N_0} P + \varepsilon \sigma P, \quad (3a)$$

$$\partial_t P + \mathbf{u} \cdot \nabla P = \mu \frac{N}{N + N_0} P - \sigma P. \quad (3b)$$

The nutrient-limited phytoplankton growth is assumed to have a maximum rate $\mu = 0.4$ d⁻¹ and a half-saturation constant $N_0 = 0.5$ mmol N m⁻³. The linear phytoplankton loss is parameterized by $\sigma = 0.1$ d⁻¹. The assumed proportion of recyclable nutrients in dead phytoplankton $\varepsilon = 0.1$. These parameter values, which are within the range of those considered in earlier works [Steidinger et al., 1998; Walsh and Steidinger, 2001; Walsh et al., 2001, 2002, 2003], result in a net population growth rate of the order of 0.25 d⁻¹ in agreement with field observations [van Dolah and Leighfield, 1999].

Equations (3) are solved using the method of the characteristics by tracing 10^4 particles, which are released every other day on a uniformly distributed lattice extending from 27°N to 26°N and from the shoreline to the 10-m isobath. Attached to each particle initially is a P -value of 0.01 mg Chl m⁻³ (the conversion equivalence for *K. brevis* is assumed be 1 mg Chl m⁻³ = 0.38 mmol N m⁻³ [Shanley and Vargo, 1993]), which is a typical background *K. brevis* concentration value on the WFS [Geesey and Tester, 1993]. Except for those particles released near the shoreline, attached to each particle initially is an

N -value of $0.1 \text{ mmol N m}^{-3}$, which corresponds to a normal oligotrophic condition on the WFS [Masserini and Fanning, 2000]. Attached to each particle released on 1 October 2004 (start date of the population dynamics model simulation) near the shoreline in the vicinity of the Caloosahatchee River initially is an N -value of 15 mmol N m^{-3} , which decays following a Gaussian function to oligotrophic initial N -values toward 13 December 2004 (end date of the population dynamics model simulation) for particles released on those intermediate dates. Attached to each particle released on 13 November 2004 near the shoreline between Estero Bay and Cape Romano initially is an N -value of 5 mmol N m^{-3} , which decays to oligotrophic initial N -values toward the start and end dates of the population dynamics model simulation for particles released on those intermediate dates.

Figure 4 shows a sequence of snapshots of the evolution of a simulated phytoplankton distribution which evolves according to (3). Note the good qualitative agreement with the observed HAB distributions shown in Figure 1, which confirms the utility of the information carried in LCSs to help identify regions of potential HAB initiation.

The results of the population dynamics model simulation are not sensitive to small variations of model parameter values or the addition of a small amount of diffusion in (3). However, they are sensitive to the location of the nutrient sources, which were revealed in the LCSs analysis, and the characteristics of these sources, which may be understood as follows. For particles released in the vicinity of the Caloosahatchee River, the assumed nonoligotrophic initial nutrient concentrations may be associated with nutrient-rich water from land runoff, which are believed to play an important role in HAB development [Brand and Compton, 2007]. The assumed nutrient concentration values and time dependence roughly adhere to measurements of, respectively, nutrient content and flow

discharge near the mouth of the Caloosahatchee River for the dates of the population dynamics model simulation. Nutrient content data and flow discharge time series are available at the U.S. Geological Survey website http://waterdata.usgs.gov/nwis/nwisman/?site_no=02292900&agency_cd=USGS. The large Caloosahatchee River flow discharges in 2004 can be attributed to a very active hurricane season. For particles released between Estero Bay and Cape Romano, the assumed nonoligotrophic initial nutrient concentrations may be associated with an upwelled intrusion of nutrient-rich GoM slope water on the WFS, which is consistent with the HYCOM simulation considered here and AVHRR (Advanced Very High Resolution Radiometer) sea surface temperature maps, e.g., <http://marine.rutgers.edu/mrs/show/?file=../regions/floridacoast/sst/noaa/2004/img/041111.316.0318.n17.jpg>. In this case, the assumed time dependence simulates the intensity variation of the upwelling event for the dates of the population dynamics model simulation.

5. Summary and Conclusions

In this paper we have traced the early stages of the development of a harmful algal bloom (HAB) produced by *Karenia brevis* which was observed on the southern portion of the West Florida Shelf (WFS) during October–December 2004. This HAB was detected offshore using ocean color imagery and field sampling. The early location of this HAB was traced with the aid of simulated Lagrangian coherent structures (LCSs). The factors that may have led to the development of this HAB were then inferred using a population dynamics model. The LCSs determine fluid particle pathways hidden in the velocity field which highly constrained the evolution of the HAB in question. To perform the LCS computation and population dynamics modeling we made use of a surface velocity

field description provided by a HYCOM (HYbrid-Coordinate Ocean Model) simulation of the WFS. With the aid of the simulated LCSs, which were identified as ridges in direct finite-time Lyapunov exponent fields, two nearshore nutrient sources were identified as responsible for the development of a simulated HAB which reproduced the main features of the event observed on the WFS in 2004. One source, which can be associated with an upwelled intrusion of nutrient-rich water on the WFS, was located in an area near the coastline between Estero Bay and Cape Romano. The other source, which can be associated with nutrient-rich water from land runoff, was located at the mouth of the Caloosahatchee River. The latter finding is consistent with the hypothesis which considers human-related nutrient loading in coastal waters as a critical factor leading to HAB development. The results of our work demonstrate that LCS simulation in combination with population dynamics modeling can greatly enhance our ability to understand the early stages of HAB development.

Acknowledgments. We are thankful to G. Halliwell and O. Smedstad for providing the HYCOM model output, M. Brown and S. Smith for critically reading the manuscript, and I. Rypina and I. Udovydchenkov for the benefit of discussions on dynamical systems theory. MJO was supported by the NSF grant CMG-0417425, the PARADIGM NSF/ONR-NOPP grant N000014-02-1-0370, the NSF grant OCE0432368, and the NIEHS grant P50 ES12736. FJBV and HK were supported by the NSF grant CMG-0417425. LEB was supported by the NSF grant OCE0432368 and the NIEHS grant P50 ES12736.

References

- Backer, L. C., et al. (2003), Recreational exposure to aerosolized brevetoxins during Florida red tide events, *Harmful Algae*, *2*, 19–28.
- Bossart, G. D., D. G. Baden, R. Y. Ewing, B. Roberts, and S. D. Wright (1998), Brevetoxicosis in manatees (*Trichechus manatus Latirostris*) from the 1996 epizootic: gross, histopathologic and immunocytochemical features, *Toxicol. Pathol.*, *26*, 276–282.
- Brand, L. E., and A. Compton (2007), Long-term increase of *Karenia brevis* abundance along the Southwest Florida Coast, *Harmful Algae*, *6*, 232–252.
- Brand, L. E., and R. R. L. Guillard (1981), The effects of continuous light and light intensity on the reproduction rates of twenty-two species of marine phytoplankton, *J. Exp. Mar. Biol. Ecol.*, *50*, 119–132.
- Chassignet, E. P., H. E. Hurlburt, O. M. Smedstad, G. R. Halliwell, P. J. Hogan, A. J. Wallcraft, R. Baraille, and R. Bleck (2007), The HYCOM (HYbrid Coordinate Ocean Model) data assimilative system, *J. Mar. Sys.*, *65*, 60–83.
- Cummings, J. A. (2005), Operational multivariate ocean data assimilation, *Q. J. Royal Meteorol. Soc.*, *131*, 3583–3604.
- de-Araújo-Carvalho, G., P. Minnett, W. Baringer, and V. Banzon (2007), Detection of Florida “red tides” from SeaWiFS and MODIS imagery, in *Anais XIII Simpósio Brasileiro de Sensoriamento Remoto*, pp. 4581–4588, Florianópolis, Brasil.
- Flewelling, L. J., et al. (2005), Brevetoxicosis: Red tides and marine mammal mortalities, *Nature*, *435*, 755–756.
- Geesey, M., and P. A. Tester (1993), *Gymnodinium breve*: ubiquitous in Gulf of Mexico waters?, in *Toxic Phytoplankton Blooms in the Sea*, edited by T. J. Smayda and

Y. Shimizu, pp. 251–255.

Green, M. A., C. W. Rowley, and G. Haller (2007), Detection of Lagrangian coherent structures in three-dimensional turbulence, *J. Fluid Mech.*, *572*, 111–120, doi:10.1017/S0022112006003648.

Haller, G. (2001), Distinguished material surfaces and coherent structures in 3D fluid flows, *Physica D*, *149*, 248–277, doi:10.1016/S0167-2789(00)00199-8.

Haller, G. (2002), Lagrangian coherent structures from approximate velocity data, *Phys. Fluids*, *14*, 1851–1861, doi:10.1063/1.1477449.

Hogan, P. J., O. M. Smedstad, J. Cummings, and A. Wallcraft (2007), Shelf break processes in the Gulf of Mexico from simulations with a Hybrid Coordinate Ocean Model, *Geophysical Research Abstracts*, *9*, 11,533.

Hu, C., F. E. Muller-Karger, C. Taylor, K. L. Carder, C. Kelbe, E. Johns, and C. A. Heil (2005), Red tide detection and tracing using MODIS fluorescence data: A regional example in SW Florida coastal waters, *Remote Sensing of Environment*, *97*, 311–321, doi:10.1016/j.res.2005.05.013.

Hu, C., F. E. Muller-Karger, and P. W. Swarzenski (2006), Hurricane, submarine groundwater discharge, and Florida’s red tides, *Geophys. Res. Lett.*, *33*, L11,601, doi:2005GL025449.

Kirkpatrick, B., et al. (2004), Literature review of Florida red tide: Implications for human health effects, *Harmful Algae*, *3*, 99–115.

Kusek, K. M., G. Vargo, and K. Steidinger (1999), *Gymnodinium breve* in the field, in the lab, and in the newspaper—A scientific and journalistic analysis of Florida red tides, *Contrib. Mar. Sci.*, *34*, 1–229.

- Landsberg, J. H. (2002), The effects of harmful algal blooms on aquatic organisms, *Rev. Fish. Sci.*, *10*, 113–390.
- Landsberg, J. H., and K. A. Steidinger (1998), A historical review of *Gymnodinium breve* red tides implicated in mass mortalities of the manatee (*Trichechus manatus* Latirostris) in Florida, USA, in *Harmful Algae*, edited by B. Reguera, M. L. Fernandez, and T. Wyatt, pp. 97–100, Xunta de Galicia and Intergovernmental Oceanographic Commission of UNESCO.
- Lekien, F., C. Coulliette, A. J. Mariano, E. H. Ryan, L. K. Shay, G. Haller, and J. E. Marsden (2005), Pollution release tied to invariant manifolds: A case study for the coast of Florida, *Physica D*, *210*, 1–20.
- Lekien, F., S. C. Shadden, and J. E. Marsden (2007), Lagrangian coherent structures in n -dimensional systems, *J. Math. Phys.*, *48*, 065,404, doi:10.1063/1.2740025.
- Lenes, J. M., et al. (2001), Iron fertilization and the Trichodesmium response on the West Florida Shelf, *Limnol. Oceanogr.*, *46*, 1261–1277.
- Masserini, R. T., and K. A. Fanning (2000), A sensor package for the simultaneous determination of nanomolar concentrations of nitrite, nitrate, and ammonia in seawater by fluorescence detection, *Mar. Chem.*, *68*, 323–333.
- Mathur, M., G. Haller, T. Peacock, J. E. Ruppert-Felsot, and H. L. Swinney (2007), Uncovering the Lagrangian skeleton of turbulence, *Phys. Rev. Lett.*, *98*, 144,502, doi:10.1103/PhysRevLett.98.144502.
- Olascoaga, M. J., I. I. Rypina, M. G. Brown, F. J. Beron-Vera, H. Koçak, L. E. Brand, G. R. Halliwell, and L. K. Shay (2006), Persistent transport barrier on the West Florida Shelf, *Geophys. Res. Lett.*, *33*, L22,603, doi:10.1029/2006GL027800.

- Riley, G. A. (1963), Theory of food-chain relations in the ocean, in *The Sea*, vol. 2, edited by M. N. Hill, pp. 438–463, John Wiley.
- Rounsefell, G. A., and W. R. Nelson (1966), Red tide research summarized to 1964 including an annotated bibliography, *U.S. Fish Will. Serv. Spec. Sci. Rep. Fish.*, 535.
- Shadden, S. C., F. Lekien, and J. E. Marsden (2005), Definition and properties of Lagrangian coherent structures from finite-time Lyapunov exponents in two-dimensional aperiodic flows, *Physica D*, 212, 271–304.
- Shadden, S. C., J. O. Dabiri, and J. E. Marsden (2006), Lagrangian analysis of fluid transport in empirical vortex ring flows, *Phys. Fluids*, 18, 47,105.
- Shanley, E., and G. A. Vargo (1993), Cellular composition, growth, photosynthesis, and respiration rates of *Gymnodinium breve* under varying light levels, in *Toxic Phytoplankton Blooms in the Sea*, edited by T. J. Smayda and Y. Shimizu, pp. 831–836, Elsevier Science.
- Shumway, S. E., S. M. Allen, and P. D. Boersma (2003), Marine birds and harmful algal blooms: sporadic victims or under-reported events?, *Harmful Algae*, 2, 1–17.
- Steidinger, K. A. (1973), Phytoplankton ecology: A conceptual review based on eastern Gulf of Mexico research, *CRC Crit. Rev. Microbiol.*, 3, 49–67.
- Steidinger, K. A., and K. Haddad (1981), Biologic and hydrographic aspects of red-tides, *BioScience*, 31, 814–819.
- Steidinger, K. A., G. A. Vargo, P. A. Tester, and C. R. Tomas (1998), Bloom dynamics and physiology of *Gymnodinium breve* with emphasis on the Gulf of Mexico, in *Physiological Ecology of Harmful Algal Blooms*, edited by D. M. Anderson, A. D. Cembella, and G. M. Hallegraeff, pp. 135–153, Springer.

- Stumpf, R. P., M. E. Culver, P. A. Tester, M. Tomlinson, G. J. Kirkpatrick, B. A. Pederson, E. W. Truby, V. Ransibrahmanakul, and M. Soracco (2003), Monitoring *Karenia brevis* blooms in the Gulf of Mexico using satellite ocean color imagery and other data, *Harmful Algae News*, 35, 1–14.
- Tester, P. A., and K. A. Steidinger (1997), *Gymnodinium breve* red tide blooms: Initiation, transport, and consequences of surface circulation, *Limnol. Oceanogr.*, 42, 1039–1051.
- Tester, P. A., R. P. Stumpf, and K. A. Steidinger (1998), Ocean color imagery: what is the minimum detection level for *Gymnodinium breve* blooms, in *Harmful Algae*, edited by B. Reguera, J. Blanco, and M. L. Wyatt, pp. 149–151, Intergovernmental Oceanographic Commission of UNESCO.
- Tomlinson, M. C., R. P. Stumpf, V. Ransibrahmanakul, E. W. Turby, G. J. Kirkpatrick, B. A. Pederson, G. A. Vargo, and C. A. Heil (2004), Monitoring *Karenia brevis* blooms in the Gulf of Mexico using satellite ocean color imagery and other data, *Remote Sensing of Environment*, 91, 293–303.
- van Dolah, F. M., and T. A. Leighfield (1999), Diel phasing of cell-cycle in the Florida red tide dinoflagellate, *Gymnodinium breve*, *Phycology*, 35, 1404–1411.
- Walsh, J. J., and K. A. Steidinger (2001), Saharan dust and Florida red tides: The cyanophyte connection, *J. Geophys. Res.*, 106, 11,597–11,612.
- Walsh, J. J., B. Penta, D. A. Dieterle, and W. P. Bissett (2001), Predictive ecological modeling of harmful algal blooms, *Human and Ecological Risk Assessment*, 7, 1369–1383.
- Walsh, J. J., K. D. Haddad, D. A. Dieterle, R. H. Weisberg, Z. Li, F. E. Muller-Karger, C. A. Heil, and W. P. Bissett (2002), A numerical analysis of landfall of the 1979 red

tide of *Karenia brevis* along the west coast of Florida, *Cont. Shelf Res.*, *22*, 15–38.

Walsh, J. J., et al. (2003), Phytoplankton response to intrusions of slope water on the West Florida Shelf: Models and observations, *J. Geophys. Res.*, *108*, 3190, doi:10.1029/2002JC001406.

Walsh, J. J., et al. (2006), Red tides in the Gulf of Mexico: Where, when, and why?, *J. Geophys. Res.*, *111*, C11,003, doi:10.1029/2004JC002813.

Wroblewski, J. S., and J. J. O’ Brien (1976), A spatial model of phytoplankton patchiness, *Mar. Biol.*, *35*, 161–175.

Wroblewski, J. S., J. L. Sarmiento, and G. R. Flierl (1988), An ocean basin scale model of plankton dynamics in the North Atlantic. 1 Solution for the climatological oceanographic conditions in May, *Global Biogeochem. Cycles*, *2*, 199–218.

Yang, H., R. H. Weisberg, P. P. Niiler, W. Sturges, and W. Johnson (1999), Lagrangian circulation and forbidden zone on the West Florida Shelf, *Cont. Shelf Res.*, *19*, 1221–1245.

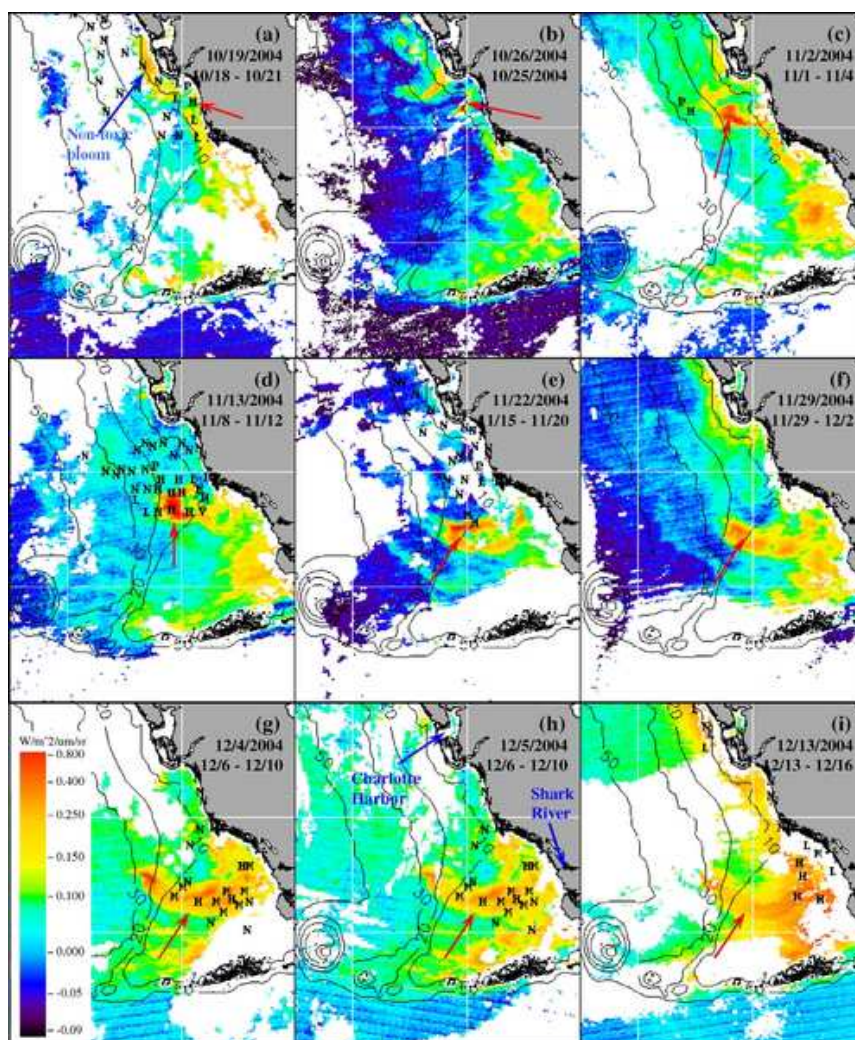


Figure 1. Sequence of MODIS (Moderate Resolution Imaging Spectroradiometer) fluorescence line height images showing the progression of a harmful algal bloom produced by *K. brevis* (indicated with red arrows) on the southern portion of the West Florida Shelf. Indicated parallels and meridians are 25°N and 26°N, and 82°W and 83°W, respectively. Superimposed on the images are water sample analysis results from the Florida Fish and Wildlife Research Institute. The second date on each image indicates the in situ sample collection time. Letters represent different *K. brevis* concentrations in cell l^{-1} as follows: N, not present or below detection limit; P, present (smaller than 10^3); L, low (between 10^3 and 10^4); M, medium (between 10^4 and 10^5); H, high (between 10^5 and 10^6); and V, very high (larger than 10^6). Reprinted from *Hu et al.* [2005] with permission. Copyright

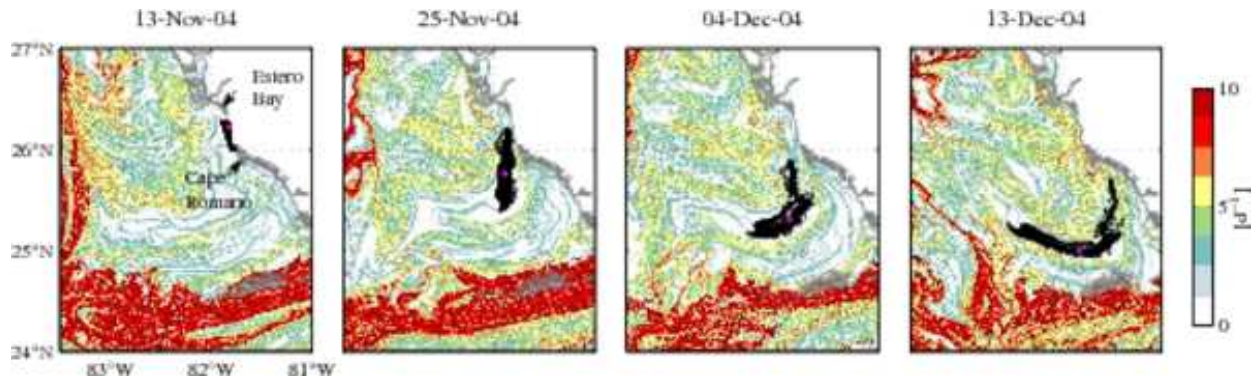


Figure 2. Snapshots of direct finite-time Lyapunov exponent (DFTLE) field (1) with initial conditions on the southern portion of the West Florida Shelf and computed backward in time using surface currents produced by a HYCOM (HYbrid-Coordinate Ocean model) simulation. Maximizing ridges of backward-time DFTLE field indicate attracting Lagrangian coherent structures (LCSs) or regions of maximum material line stretching toward which fluid particles converge as time progresses. These LCSs are hidden in the velocity field and thus cannot be inferred visually from snapshots. The clouds of black dots with the magenta dot immersed indicate simulated passively advected particles. These were used, as explained in the text, in tracing the early development of a simulated harmful algal bloom (HAB), whose evolution is shown in Figure 4, which reproduces the main characteristics of the observed HAB shown in Figure 1.

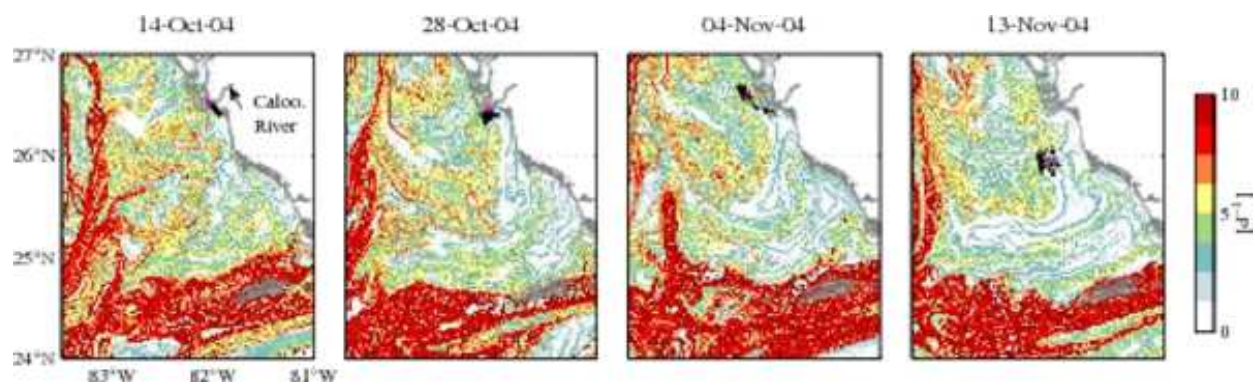


Figure 3. As in Figure 2, but for a different set of dates. Indicated in the left panel is the Caloosahatchee River, which has been abbreviated as Caloo. River.

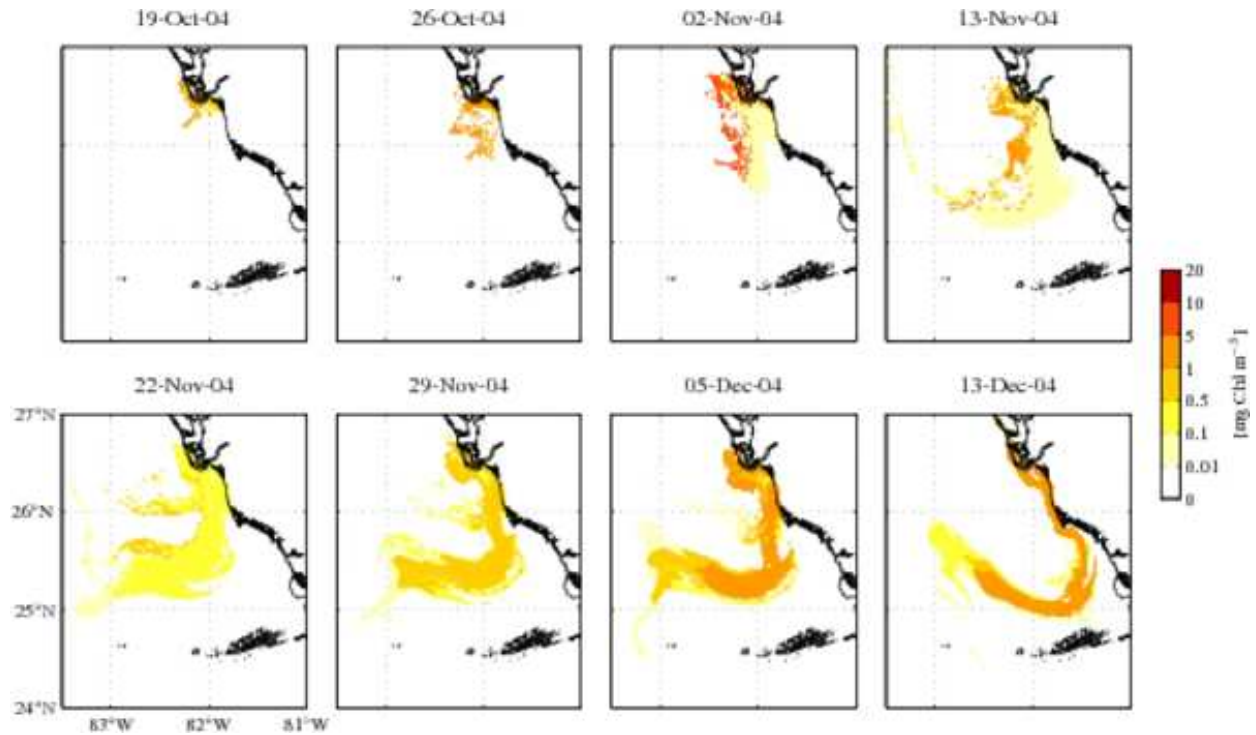


Figure 4. Series of snapshots of the evolution of a harmful algal bloom (HAB) produced by *Karenia brevis* on the southern West Florida Shelf as simulated according to (3) using a HYCOM (HYbrid-Coordinate Ocean model) based surface current description and the fluid particle motion information carried in the Lagrangian coherent structures shown in Figures 2 and 3. The simulated HAB reproduces the main features of the observed HAB shown in Figure 1.